NUMERICAL SIMULATION AND ANALYSIS OF DROPLET IMPACTING A HEATED WALL BASED ON VOF

Yunfei KOU[1], Rujun WU[2], *Yifei GUI[3]

In this paper, the process of droplet impacting a high-temperature wall is numerically simulated using STARCCM+ software based on the VOF method. The effectiveness of this simulation method is verified by comparing it with experimental results.The results show that under the same conditions, the higher the initial velocity of the droplet when it impacts the wall, the shorter the time required for the droplet to reach boiling evaporation after impacting the wall, and the faster the evaporation rate of the droplet. A smaller contact angle is more conducive to rapid heating and evaporation of the droplet, while a larger contact angle may cause the droplet to bounce off, reducing heat transfer.

Keywords: VOF; numerical simulation; droplet impact on high-temperature wall; boiling evaporation

1. Introduction

After contact with a high-temperature wall, water droplets absorb heat and vaporize, producing water vapor and cooling the wall surface. This process greatly improves heat transfer efficiency. Due to its high heat and mass transfer capacity, this effect is widely used in petroleum, chemical, metallurgical, energy, and other fields.On the one hand,The impact of water droplets can enhance their cooling effect on the wall surface, such as in spray cooling [1, 2], which has the advantages of being easy to implement, enhancing heat transfer capacity. It has been widely applied in the microelectronics industry, steel rolling, metal casting, fine water mist fire suppression, and other fields. On the other hand, droplet impact may also have adverse effects on some industrial equipment. For example, in steam turbines, the superheated steam works by gradually expanding, so its pressure continues to decrease, and after reaching the saturation zone, the steam gradually condenses into tiny droplets, which in turn leads to blade wear, thereby endangering the safe operation of the device [3].Meanwhile, in internal

* Corresponding author

[1] Yunfei Kou, School of Mechanical, Shanghai DianJi University，China, e-mail: 1981850715@qq.com

[2] Rujun Wu, School of Mechanical, Shanghai DianJi University, China, e-mail: correspondingshdj@163.com

[3] Yifei Gui, School of Mechanical, Shanghai DianJi University, China, e-mail: guiyf@sdju.edu.cn

combustion engines, there is also a phenomenon of droplets impacting and heating walls[4], ion sputtering, and other fields.The phenomenon of droplets impacting a heated wall has attracted scientists to continue research and provide scientific explanations because it exists everywhere in industrial technology. Chandm et al. and Chandra [5] conducted experimental research on the impact of n-heptane droplets on a heated wall and found that three phenomena occur after the droplets impact the wall as the initial wall temperature changes.

The phenomenon of Leidenfrost was first described by Leidenfrost [6], in which liquid droplets adhere to a hot wall. As the temperature of the wall increases, a vapor film gradually forms on the contact area between the droplet and the wall, preventing the droplet from making direct contact with the wall.At this point, the droplet remains suspended, even completely detached from the wall, and as the evaporation time increases, the droplet evaporation time is longest when the wall temperature reaches the Leidenfrost temperature.Anders et al. [7] arrived at this conclusion by varying the impact velocity and diameter of ethanol droplets, and found that if the wall temperature exceeds the Leidenfrost temperature, droplets corresponding to larger we numbers will assume irregular shapes, and if the we number exceeds a critical value, the droplets will break up, forming a large number of secondary droplets.Zhang et al. [8] found that the evaporation pattern of droplets containing particulate matter is constant within the contact radius, and the dried droplets leave a ring of particles on the surface of the solid substrate.It is generally believed that the droplet is spherical cap-shaped [9].For the volume of a droplet on a wall, it can be obtained by the droplet height h, contact radius r, contact angle θ, and the radius of the sphere, as follows:

$$R = Rsin\theta \tag{1}$$

$$h = \left(1 - Rcos\theta\right) = rtan\left(\theta/2\right) \tag{2}$$

$$V = \frac{\pi r^3\left(2 - 3cos\theta + cos^3\theta\right)}{3sin^3\theta} \tag{3}$$

$$A_{SL} = \pi R^2 \tag{4}$$

In the equation, V is the volume of the liquid, and A_{SL} is the area of the solid-liquid interface.

Gottfred et al. [10], Wachters et al. [11], and Kenneth et al. [12] established mathematical models for early droplet changes in the film boiling region, which can analyze the thickness of the vapor film and obtain the evaporation rate of the droplets.Based on these mathematical models, it is possible to address special cases, such as wall roughness [13, 14].Sen and Black [15] first theoretically analyzed the energy conservation equation of spherical droplets in polar coordinates.

2. Models and Methods

2.1 Computational Model

A three-dimensional model as shown in Fig 2.1 was established for the simulation calculation of droplet impact on a wall surface. The calculation domain is a cube with length, width, and height of 15 millimeters, with the bottom set as the wall surface and the remaining five faces set as symmetrical planes. The use of symmetrical planes can reduce the introduction of errors due to non-physical boundary conditions, such as inaccurate treatment of completely enclosed or open boundaries, which can lead to instability of simulation calculation.

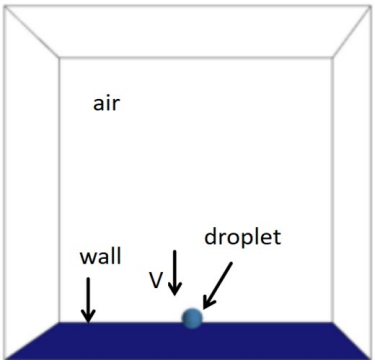

Fig 2.1 3D model of fluid domain

To avoid numerical errors caused by asymmetry, the symmetric domain simplifies the computational model and improves research efficiency (velocity, droplet size) or wall parameters (e.g., temperature, contact angle) when conducting parametric studies on the initial conditions of droplets. The simplified geometric shape facilitates the analysis of physical phenomena related to the interaction of simulation calculation.

2.2 Parameter and boundary settings

The computational fluid is air and water, with the bottom set as a wall, the perimeter and top as symmetrical planes to reduce the introduction of non-physical boundary conditions. The thermal specification for the bottom is set to temperature, and the wall specification is selected as smooth, as the no-slip condition allows the calculation of the velocity gradient of the boundary layer, which helps accurately capture the velocity distribution and shear stress near the wall. Therefore, the shear stress specification is selected as no-slip. The initial shape of the droplet is spherical.

2.3 Governing Equations

(1) Energy conservation equation

In multiphase flow simulations involving heat transfer (such as droplet impact on a wall resulting in changes in wall temperature), the energy

conservation equation can be expressed by applying the first law of thermodynamics to the control volume:

$$\frac{\partial(\rho \mathrm{E})}{\partial t}+\nabla \cdot(\rho \mathrm{E} \nu)=f_b \cdot \nu+\nabla \cdot(\nu \times \sigma)-\nabla \cdot \mathrm{q}+\mathrm{S}_{\mathrm{E}} \quad (5)$$

E is the total energy per unit mass, in joules per kilogram (J/kg), and q is the heat flux, in watts per square meter (W/m^2); typically, it is the volumetric energy source term, in watts per cubic meter (W/m^3).

(2) Momentum conservation equation (Navier-Stokes equation)

The rate of change of momentum of a continuous medium is equal to the resultant external force acting on the continuous medium. In multiphase flow, interphase forces (such as surface tension) need to be considered. This equation can be expressed as:

$$\frac{\partial(\rho v)}{\partial t}+\nabla \cdot(\rho \vec{v} \times \vec{v})=\nabla \sigma+f_b \quad (6)$$

σ is the surface tension, in N/m, and is the resultant force of the volumetric forces (such as gravity and centrifugal force) acting on a unit volume of a continuous medium, in N (newtons).

(3) Continuity equation (mass conservation)

For multiphase flow, to describe the conservation of mass of the fluid, it is necessary to consider the mass fraction or volume fraction of each component. The continuity equation is used to express the mass balance relationship of the control volume, as follows:

$$\frac{\partial \rho}{\partial \mathrm{t}}+\nabla \cdot(\rho \mathrm{v})=0 \quad (7)$$

ρ is the density, which is the mass per unit volume, with the unit of kg/m^3; v is the velocity of the continuous medium, with the unit of m/s; and t is time, with the unit of second (s).

2.4 Model and method validation

In the simulation software, the Physical models can simulate the real process of droplets colliding with a wall. The specific three-dimensional model settings of the fluid domain volume can be seen in Fig 2.1 above. The simulation process uses a volume-of-fluid(VOF) method, which is a numerical method used to simulate multiphase flows. It is particularly adept at handling situations with clear, sharp interfaces between immiscible fluids. Its core idea is to track the clear interfaces between immiscible fluids by solving the volume fraction of each grid cell.To verify the reliability of the method and the selected model, this paper conducted a simulation study on the experimental research results of the dynamic process of bubble-containing droplets impacting a wall surface in the literature by Gulyaev et al. [16], verifying the reliability and accuracy of the method from both quantitative and qualitative aspects.

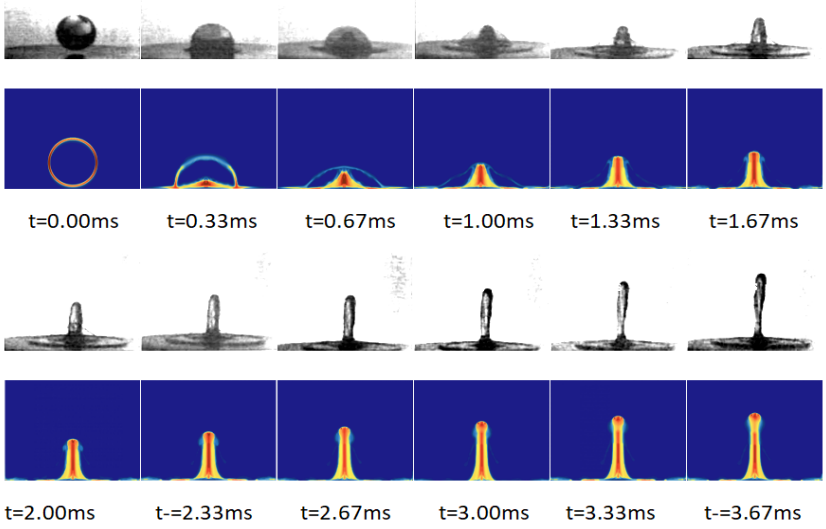

(a) Qualitative comparison between experimental results and simulation results

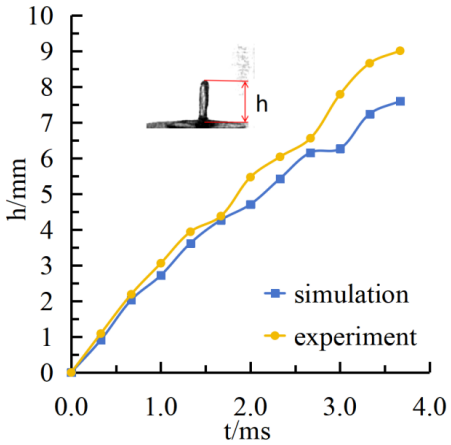

(b) Qualitative comparison between experimental results and simulation results

Fig 2.2 Comparison of simulation results and experimental results

Fig 2.2 shows the comparison between experimental results and simulation results. The droplet diameter is 5.25mm, the internal bubble diameter is 4.82mm, and the droplet impact velocity on the wall is 5.94m/s.From Fig 2.2(a), it can be observed that the numerical simulation results are consistent with the experimental results in the literature, both showing the phenomenon of droplets spreading laterally on the wall and jetting occurring, and the change trend at each moment is also relatively consistent. Furthermore, from Fig 2.2(b), it can be seen that the simulation results of the jet height are also very close to the experimental results.The simulation results of jet height at each moment are only slightly smaller than the experimental results. The comprehensive analysis of the reasons

should be: the experimental conditions measured in the literature are experimental results, and there will definitely be errors in the actual instrument measurements. Another reason is that the simulation conditions and experimental factors at that time cannot be exactly the same.There are also certain limitations in the image processing techniques, but overall, this numerical simulation method can accurately simulate the dynamic motion process of droplets impacting the wall surface.

2.5 Grid-independent verification

As shown in Fig 2.3, this paper verifies the total number of grids with six different densities: 201,400, 397,600, 604,800, 807,600, 900,300, and 1,988,100. The variation of the droplet spreading coefficient with time is observed when a 1mm water droplet impacts a high-temperature wall surface at 573k,where the spreading coefficient β is defined as,$\beta=D_0$ is the initial diameter of the droplet, and is the maximum spreading diameter of the droplet on the wall. From the Fig, it can be seen that when the number of grids reaches 800000, the change in spreading coefficient tends to be stable, and the grid number corresponds to 807,600. The diffusion coefficient error for 1,988,100 is 0.43%, which can be neglected. This grid number is reliable, so the grid number of 807600 is selected for simulation.

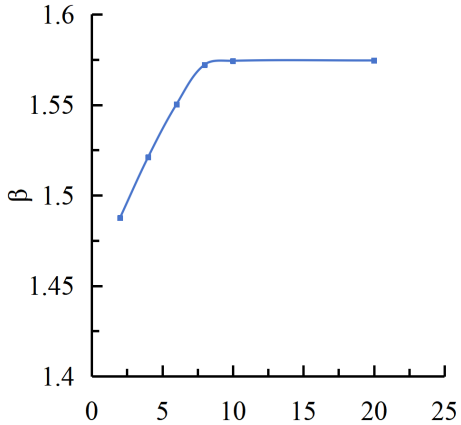

Fig 2.3 Grid Independence Verification(number of grids×10^4)

3. Results and Analysis

3.1 Simulation results and analysis of spreading coefficients of droplets with different diameters

3.1.1 Simulation Parameters

The droplet diameter plays a crucial role in the impact of droplets on the wall surface, directly affecting the dynamic behavior of droplets, including spreading, rebounding, breaking and evaporation. Numerical simulations were conducted on

the process of droplets with different diameters impacting a wall surface with a contact angle of 120° at a speed of v=1m/s, with the surface tension coefficient set to 0.072N/m.

As shown in Fig 3.1, when the droplet size ranges from 0.5 mm to 1.5 mm, the variation of the droplet diffusion coefficient during the spreading process when it impacts a high-temperature wall can be observed. From the change in diffusion coefficient in the Fig, it can be seen that the droplet rapidly diffuses after impacting the wall surface, and the kinetic energy of the droplet is continuously converted into surface energy. There is also viscous dissipation energy on the wall layer, which is the process of interaction between inertial force, viscous force, and surface tension. When the three reach equilibrium, the droplet reaches its maximum spreading area and begins to contract, and the spreading coefficient decreases accordingly.After repeated spreading and contraction, the maximum spreading coefficient of the droplet decreases as the energy is continuously consumed. When the total energy reaches the minimum surface energy of the droplet, the droplet tends to be stable. It can be observed that when the droplet diameter is too large, the surface of the droplet will rupture due to the excessive inertial force of the droplet, forming a series of small droplets. For example, in the simulation, 1.25mm and 1.5mm water droplets will undergo droplet wall collision and rupture.

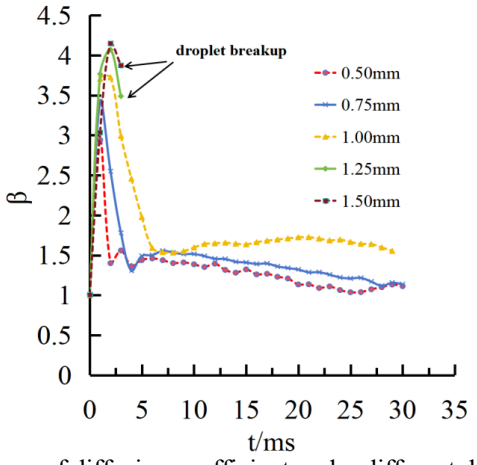

Fig 3.1 Change of diffusion coefficient under different droplet diameters

After hitting the wall, the droplet reaches its maximum spreading area in a very short time. droplets with diameters of 0.5mm, 0.75mm, and 1.25mm can achieve maximum spreading diameters of 2.9 times, 3.4 times, and 3.7 times their own diameters, respectively. The time intervals for them to reach their maximum spreading areas are not very different. As the kinetic energy and surface energy of the droplet continue to be converted, viscous dissipation continuously reduces the total energy, and the area of each contraction of the droplet becomes smaller and smaller, eventually reaching an equilibrium state. Among them, droplets with

diameters of 1.25mm and 1.5mm can achieve maximum spreading diameters of about 4.1 times their own diameters, but they will quickly break up after reaching their maximum spreading area.

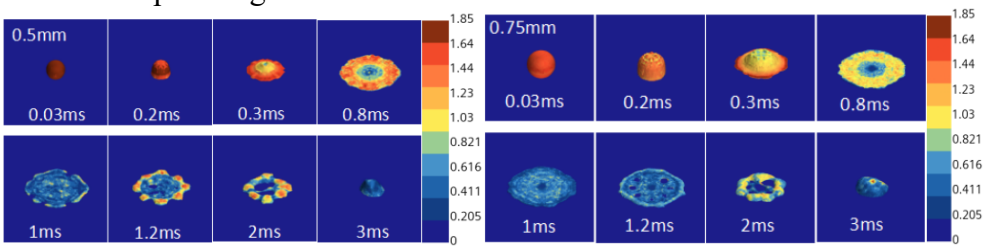

(a)

(b)

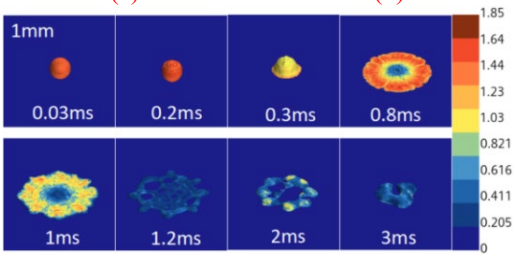

(c)

As can be seen from Fig 3.2(a, b), droplets with diameters of 0.5 mm and 0.75 mm gradually spread into a snowflake shape, and their edges formed some small droplets around them, which then gradually retracted after spreading to its maximum extent. Droplets with a diameter of 1 mm also formed small droplet at the edge after impacting the wall and diffusing and retracting. The droplet broke internally, and as it continued to retract, the cracks inside the droplet became larger and larger. Due to the continuous consumption of energy, the degree of spreading of the droplet also continued to decrease.For droplets with diameters of 1.25mm and 1.5mm, due to the larger droplet diameter, after the droplet hits the wall and diffuses, the edge and interior of the droplet break at around 3ms, This makes it impossible to measure the spreading coefficient of the droplet after it has reached its maximum spreading state, as shown in Fig 3.2(d, e). This is consistent with the curve changes in Fig 3.1.

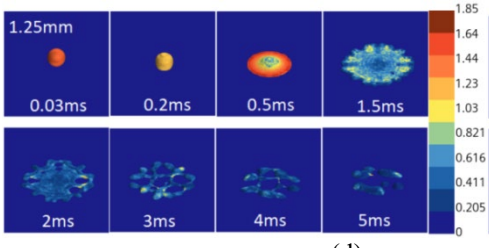

(d)

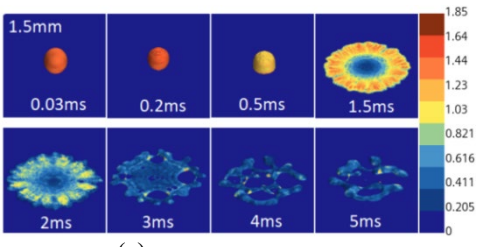

(e)

Fig 3.2 Velocity field diagram of droplets of different sizes impacting the wall surface

It can be seen that larger droplets have higher kinetic energy and greater inertial forces during the spreading process, which may lead to excessive spread

or even breakage. Surface tension has a more pronounced effect on small droplets, making them easier to maintain integrity. Since the simulated wall temperature is set at 573K, the larger the droplet, the larger the heated area on the high-temperature wall, resulting in uneven internal heat transfer and forming a strong temperature gradient, making the droplet more likely to break during evaporation.

3.1.2 Temperature field analysis

The temperature field of a droplet impacting a high-temperature wall is shown in Fig 3.3. At the beginning, both the droplet and the air region are maintained at 300K. As the droplet diffusion process progresses, it can be seen from the Fig that the droplet contacts the wall surface in a short period of time, and the temperature of the droplet does not rise rapidly. The heat transfer that occurs is mainly between the wall surface and the surrounding air. It can be seen that the temperature of the air near the wall surface continues to rise with time, and the temperature is higher the closer it is to the wall surface,The main reason is that the specific heat capacities of air and water differ significantly. The specific heat capacity is represented by the height unit of a unit mass of substance. The specific heat capacity of air is approximately 1.03x103J/(kg/K), while the specific heat capacity of water is approximately 4.2×103J/(kg/K), so the specific heat capacity of water is approximately four times that of air. Moreover, at the same temperature, the amount of heat absorbed by water is much greater than that absorbed by air. Therefore, the temperature of air near the wall surface is much higher than that of water droplets.

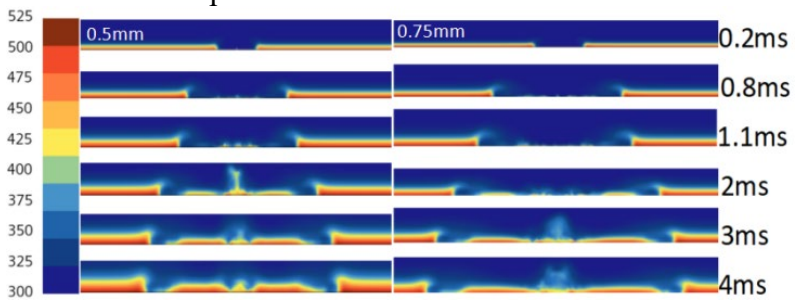

(a) (b)

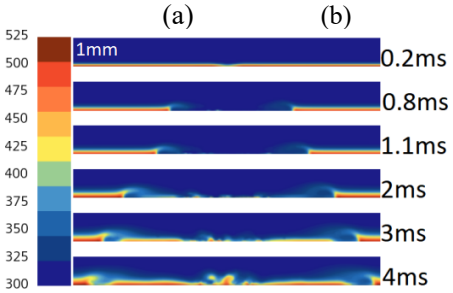

(c)

As shown in Fig 3.3(a, b), it is worth noting that when the droplet diameter is 0.5 mm and 0.75 mm, due to the limited volume of the liquid, the diameter of the

spreading liquid film is smaller, and the area of the wall temperature reduction is smaller.

As shown in Fig 3.3, the droplet diameters are 0.5mm, 0.75mm, 1 mm, 1.25 mm, and 1.5 mm, respectively. When the droplet impacts the high-temperature wall, due to the large volume of the bottom of the droplet, the upper layer remains at a lower temperature for a short period of time after the droplet impacts the wall, forming a temperature gradient. This can be clearly seen from the temperature field diagram after the droplet impacts the wall in Fig 3.4.Due to the increase in temperature at the bottom after spread out, while the temperature at the top remains low, the uniformity of heating is generally poor. Furthermore, as can be seen from the temperature field diagram in Fig 3.3, the smaller the droplet diameter, the faster the droplet spreads and retracts, resulting in a thinner liquid film thickness and a faster rate of temperature rise in the liquid film. This is consistent with the trend of temperature variation with time for droplets of different sizes after impacting the wall in the temperature field diagram in Fig 3.4.

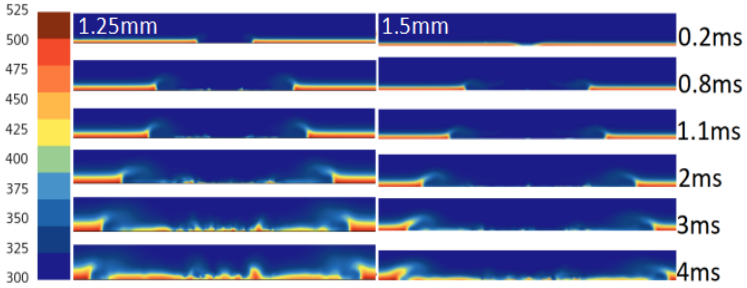

(d) (e)

Fig 3.3 Wall temperature field diagram of different size droplets impacting the heated surface

As can be seen from Fig 3.3, the spreading diameter of droplets with smaller diameters after impacting the wall is relatively small, reducing the direct contact area between the droplets and the wall, reducing heat transfer efficiency, and delaying evaporation rate. As shown in Fig 3.5, the evaporation rate is very low.At the onset of diffusion, heat transfer is relatively slow, potentially experiencing a prolonged evaporation phase, aligning with the evaporation rates of smaller droplets depicted in Fig 3.5. As droplet size increases, some liquids may undergo explosive evaporation in short time. The initial contact area between the droplet base and the wall is larger, with more liquid in direct contact with the wall compared to smaller droplets. Consequently, it absorbs more heat from the wall and facilitates more efficient heat transfer than smaller droplets. This aligns with the evaporation rates of droplets with diameters of 1.25 mm and 1.5 mm shown in Fig 3.5.

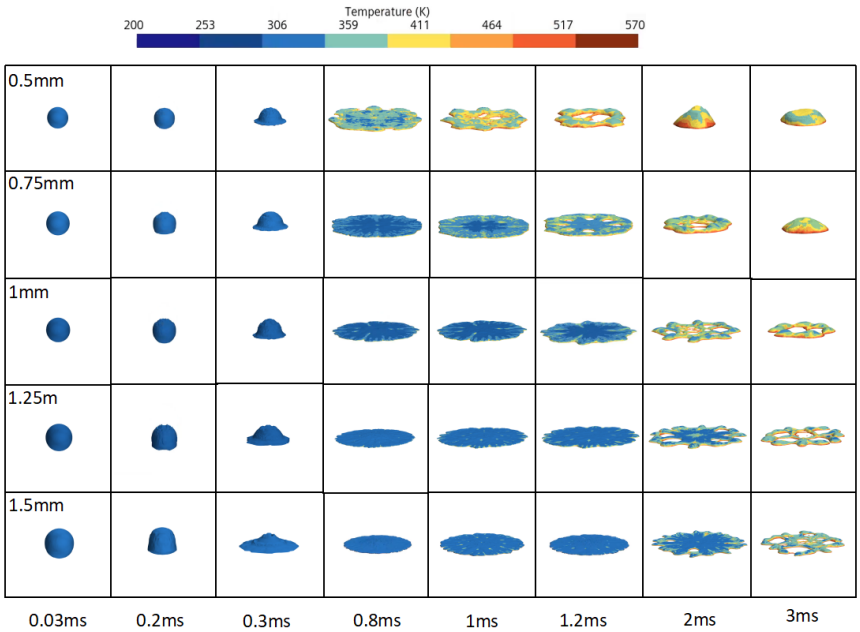

Fig 3.4 Temperature field diagram of droplets with different sizes impacting the wall surface

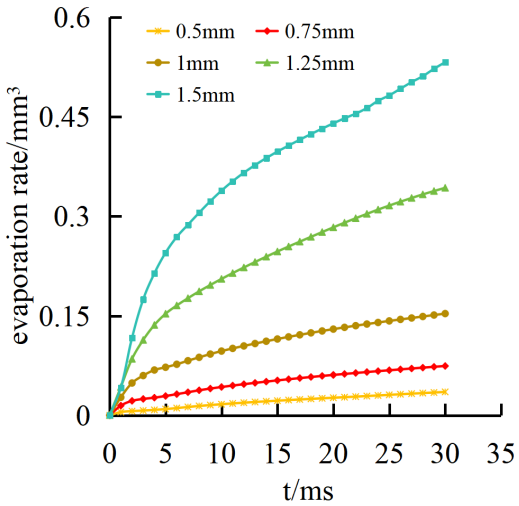

Fig 3.5 Schematic diagram of the rate of water vapor generation when droplets of different sizes impact a high-temperature wall

As shown in Fig 3.5, from top to bottom are water droplets of five sizes: 0.5 mm, 0.75 mm, 1 mm, 1.25 mm, and 1.5 mm, generated after hitting the wall. The slope represents the evaporation rate of the water droplets. From the Fig, we can see the evaporation rates of the five types of water droplets from top to bottom.

Due to the small droplet size of 0.5 mm, it quickly evaporates after hitting the wall and heating, with a low evaporation rate and small water vapor release. Droplets with diameters of 0.75 mm and 1 mm release more water vapor than 0.5 mm droplets after hitting the wall due to their greater spreading extent. The largest

droplets evaporate the most violently, with a faster evaporation rate and the highest water vapor release.

3.2 Simulation results and analysis of spreading coefficient under different wall contact angles

3.2.1 Analysis of simulation parameters and droplet spreading

The wall contact angle has a significant impact on the diffusion, rebound, evaporation, and breakup behavior of droplet impact the wall. The morphology of the droplet on the wall is determined by the dynamic changes in contact angle. A smaller contact angle promotes diffusion and evaporation, while a larger contact angle leads to rebound and splash. This section numerically simulates the process of a water droplet with a diameter of 1 mm impacting a wall at room temperature at a speed of v=1m/s under different static contact angles. The surface tension coefficient is set to 0.072N/m. From the five curves in Fig 3.6, it can be seen that the droplet impact flow process is closely related to the wettability of the wall. At the initial stage of spreading, the spreading coefficient decreases correspondingly as the wall contact angle increases.

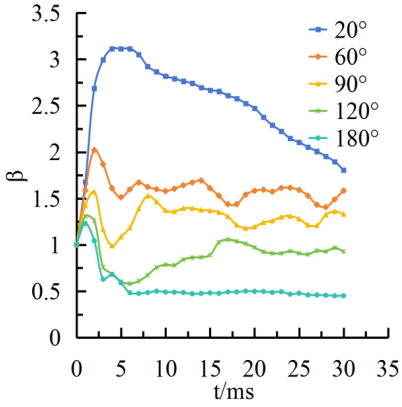

Fig 3.6 Change of spreading coefficient of droplet impacting wall under different wall contact angles

As shown in Fig 3.7(a), when the wall contact angle is 20°, the droplet reaches its maximum diffusion at 6ms after impacting the wall. The speed and tendency of the droplet to retract are minimal. Due to the small tendency to retract, the droplet cannot store enough kinetic energy to rebound. Eventually, after a slow retraction of more than 20 milliseconds, the droplet spreads out on the wall in a large area of liquid film, unable to produce a rebound phenomenon.

As shown in Fig 3.7(b, c, d), during the subsequent contraction phase, as the wall contact angle increases, the degree of spreading of the droplet after impacting the wall is smaller at wall contact angles of 60°, 90°, and 120° compared to a contact angle of 20°, and a preliminary rebound phenomenon begins to occur.

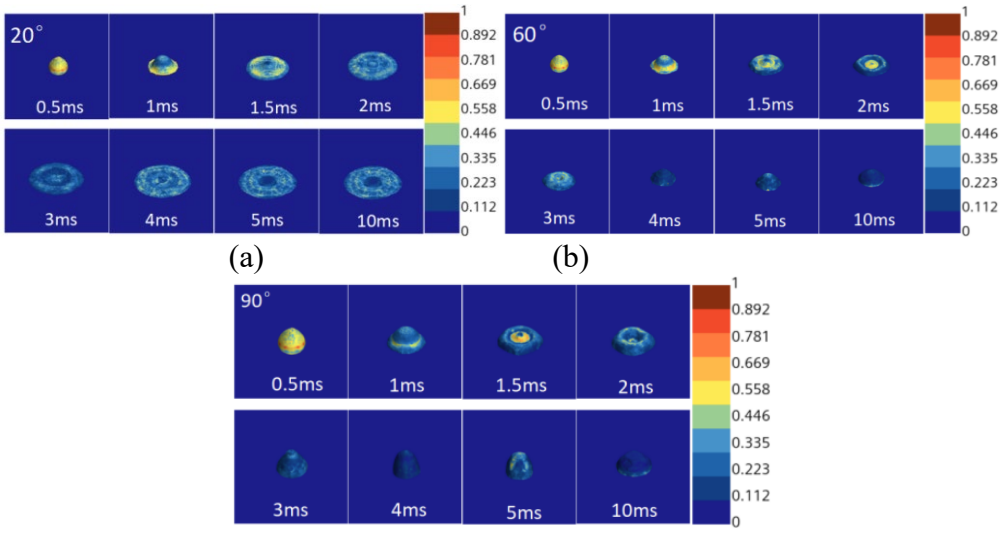

For 180 ° superhydrophobic wall, droplets do not "stick" to the surface after impact. Droplets tend to reduce their contact area with the wall and maintain a spherical shape, thereby reducing kinetic energy loss and making it easier to retract and rebound. However, during the upward rebound process, the droplet do not completely detach from the wall after reaching a certain height. As shown in Fig 3.7 (e).

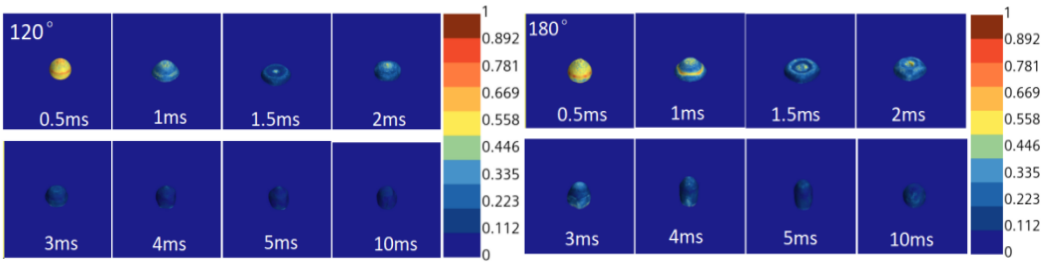

Fig 3.7 Velocity Field of Droplet Impact on Wall at Different Wall Contact Angles

The results indicate that The changes in the form of water droplets varies under different wetting conditions. Inertia, viscosity, surface tension, and wall adhesion are the main affecting factors. Inertial force will keep the droplet in its current flow state, viscosity will prevent the droplet from moving, and surface tension will keep the droplet in the state of minimum surface area.

Research has found that during the process of droplet impact, the droplet gradually spreads under the action of inertia. The smaller the wall contact angle, the higher the wall hydrophilicity, making the droplet easier to spread. Conversely, the smaller the wall contact angle, the less likely it is to spread.

Then, due to the influence of surface tension and viscosity of the droplet, the droplet begins to contract when it reaches its maximum spreading diameter. During the contraction process, the larger the wall contact angle, the greater the hydrophobicity of the wall, the smaller the adhesion force, and the easier it is for the droplet to contract and rebound.

3.2.2 Temperature Field Analysis

The smaller the contact angle between the droplet and the wall, the larger the contact area between the droplet and the wall, and the larger the diffusion diameter. The heating speed at the bottom of the droplet is fast, the internal temperature gradient is large, and the center temperature of the droplet is relatively low.Due to the large contact area between the droplet and the wall, the efficiency of heat transfer from the wall to the droplet is higher, and the evaporation rate of the droplet is relatively fast. Especially at a contact angle of 20 °, the droplet rapidly thins and eventually evaporates completely. This can be seen in Fig 3.8 (a).

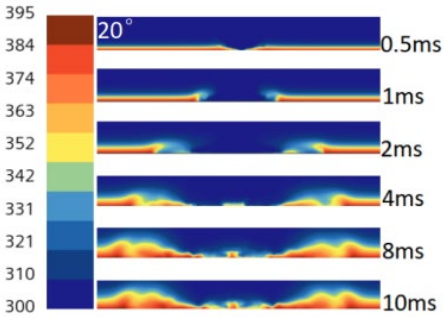

(a)

As shown in Fig 3.8 (b), when the wall contact angle exceeds 60 °, the droplet is in a moderately spreading state, with a relatively uniform temperature gradient. The temperature at the bottom of the droplet is relatively high and gradually decreases upwards. Compared with low contact angle, the contact area is slightly smaller and the heat transfer efficiency is moderate. The evaporation rate is moderate, and the droplets remain relatively stable for a long time.

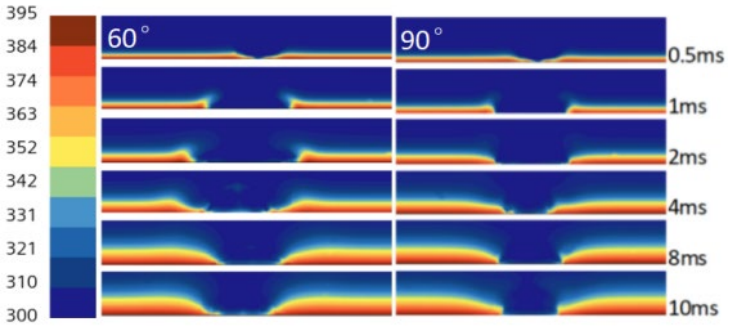

(b) (c)

As the contact angle between the droplet and the wall increases, the contact area between the droplet and the wall significantly decreases, and the droplet becomes approximately spherical. This phenomenon can be clearly observed from the temperature field diagram of the droplet hitting different wettable walls in Fig 3.9. The temperature gradient inside the droplet is low, and the heat is mainly concentrated at the bottom of the droplet, making it difficult to quickly conduct to the upper part of the droplet. Due to the small contact area and low heat transfer efficiency, the range of local temperature drop on the wall is relatively small, as shown in Fig 3.8 (c, d, e). Droplets may partially retract or even rebound, resulting in limited evaporation and low evaporation rate.

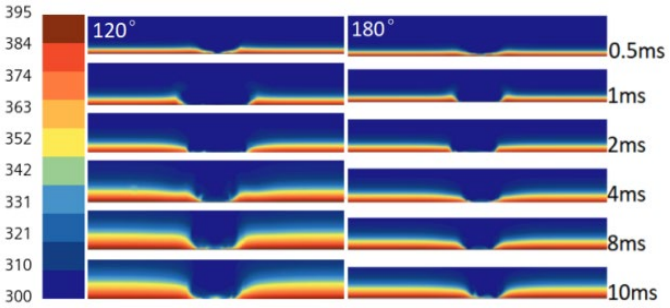

(d) (e)

Fig 3.8 Wall Temperature Field of Droplet Impact on Wall at Different Wall Contact Angles

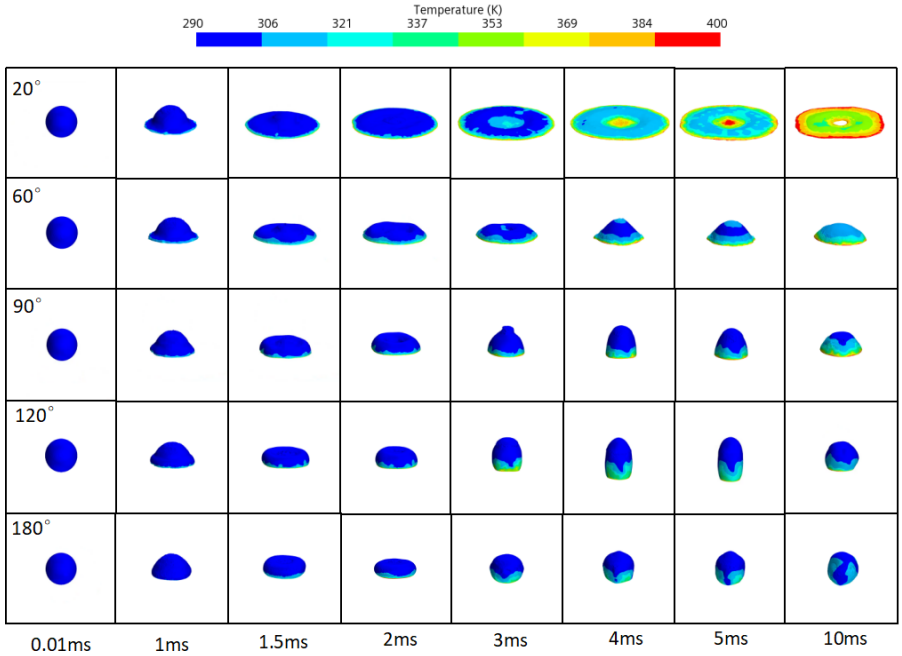

Fig 3.9 Temperature Field of Droplets Impacting Different Wettability Walls

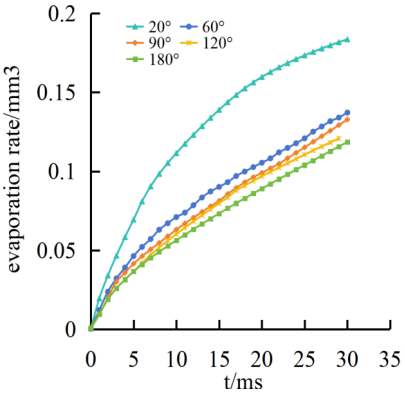

Fig 3.10 Schematic diagram of water vapor generation rate of droplet impact on high-temperature wall at different wall contact angles

3.3 Simulation results and analysis of droplets with different physical properties colliding with wall surfaces

3.3.1 Simulation Parameters and Spread Analysis

This article also conducted simulation studies on the motion process of droplets with different physical properties hitting walls, in order to compare whether the motion laws of droplets with different physical properties hitting walls with different wetting properties are the same. Therefore, two liquids, diesel and water, were selected for simulation comparison. The droplet diameter was 1mm, the wall temperature was 573k, the droplet impact wall velocity was v=1m/s, and the wall contact angles were 20 °, 90 °, and 180 °, respectively.

From Fig 3.11, we can see that the trend of the spreading of small diesel droplets and water droplets hitting the wall surface with different contact angles is roughly consistent over time, and under the same conditions, the maximum spreading coefficient of water droplets is slightly larger than that of diesel droplets. Moreover, the spreading change pattern of diesel droplets hitting the wall surface is consistent with that of water. The larger the wall contact angle, the smaller the maximum spreading area of the droplets. A special phenomenon is that when diesel droplets hit the wall surface at a contact angle of 180 °, there is a brief rebound of the droplets from the wall surface,The reason can be attributed to the formation of a vapor film buffer layer between the droplet and the high-temperature wall. Due to the strong rebound tendency of the droplet on the superhydrophobic wall, under the combined action of the thrust generated by the vapor film, diesel droplets collide with the high-temperature wall and rebound away from it.

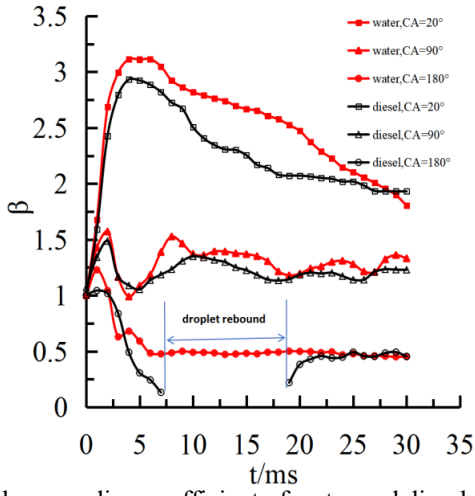

Fig 3.11 Changes in the spreading coefficient of water and diesel droplets hitting the wall at different contact angles

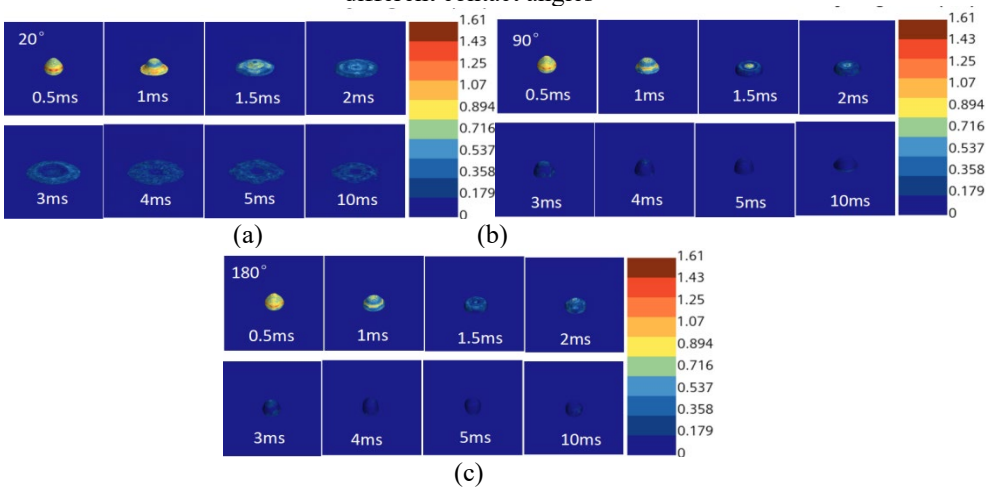

Fig 3.12 Velocity Field of Diesel Droplet Impact on Walls with Different Wettability

3.3.2 Temperature Field Analysis

From the temperature field diagram of diesel droplets hitting the wall, it can be seen that when the droplets hit the wall at a 20 ° contact angle, the droplets spread more fully, the resulting liquid film is thinner, and the contact area with the wall is larger. Therefore, the droplets rise faster at night. In contrast, the droplet heating rate is slower at a 90 ° wall contact angle, and the droplet heating rate is slowest at a 180 ° wall contact angle. At different contact angles, the evaporation rate of diesel droplets is also the fastest at a 20 ° contact angle, slower at a 90 ° wall contact angle, and slowest at a 180 ° wall contact angle.However, from the evaporation rate chart of diesel and water in Fig 3.14, it can be seen that under the same contact angle conditions, the evaporation rate of diesel droplets is much faster than that of water. And diesel droplets, like water droplets, have a smaller

contact angle with the wall surface, better clarity on the wall surface, stronger tendency to spread at night, and faster liquid evaporation rate.

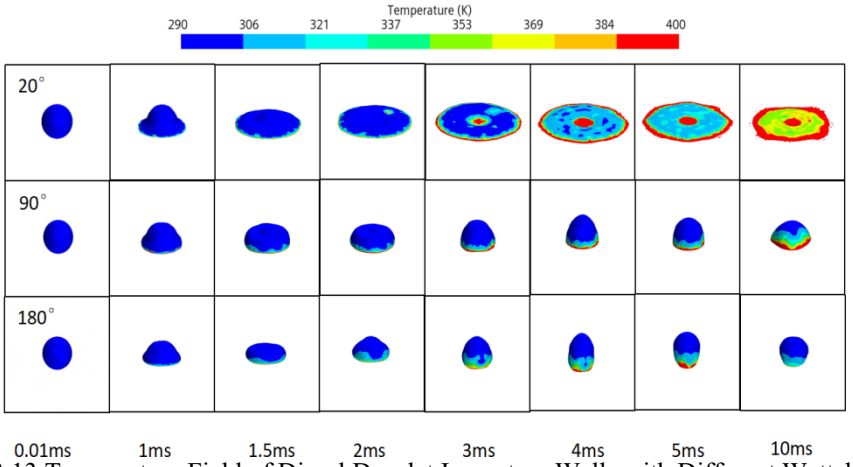

Fig 3.13 Temperature Field of Diesel Droplet Impact on Walls with Different Wettability

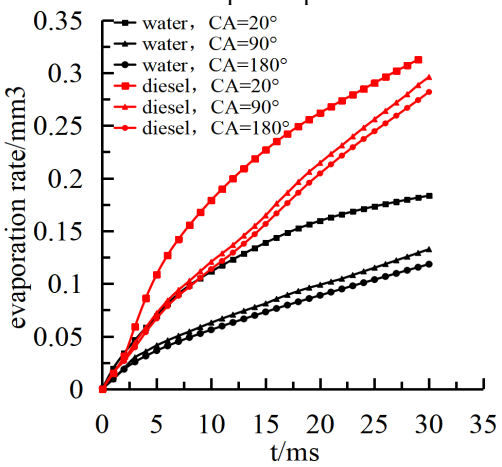

Fig 3.14 Schematic diagram of water vapor generation rate when water and diesel droplets collide with high-temperature walls at different wall contact angles

One of the more unique phenomena is that the boiling point of diesel is generally around 210 ℃, while the boiling point of water is about 100 ℃. From the simulation results, under the same conditions, the evaporation rate of diesel is much faster than that of water. This can be explained by the fact that water is more prone to boiling than diesel, while water has more hydrogen oxygen bonds between molecules and stronger intermolecular forces, making it difficult to evaporate. Conversely, although diesel has a higher boiling point, the intermolecular forces are weaker and the evaporation rate is faster. The trend of this change can be clearly observed from Fig 3.14.

4. Conclusion

1. When droplets collide with a wall, they will diffuse, contract, or rupture. Due to the large inertia effect, the larger the droplet size, the larger the final spreading diameter. Due to the large inertia force of large-sized droplets, the spreading rate is also high. However, droplets with excessively large diameters are prone to rupture after reaching the maximum spreading diameter, as shown in the droplets with diameters of 1.25mm and 1.5mm in Fig 3.1.
2. Droplets with smaller diameters have smaller volumes and smaller contact areas with the wall, which reduces heat transfer efficiency and slows down evaporation rate. Due to the wall temperature of 573K being much higher than the boiling point of water, droplets begin to evaporate violently at the moment of impact. Due to the intense evaporation, it may promote the formation and rupture of large droplets, resulting in a shortened droplet spreading time, especially for large droplets that may be affected by evaporation.
3. Generally speaking, a smaller contact angle is more conducive to rapid heating and evaporation of droplets, while a larger contact angle may cause droplet rebound and reduce heat transfer. From Figs 3.9 and 3.10, it can be seen that the droplet spreading coefficient is larger on the wall at a 20 °contact angle, while the maximum spreading area of the droplet does not change much and is relatively small relative to the wall at contact angles of 60 °, 90 °, 120 °, and 180 °.For industrial applications such as cooling and efficient evaporation, wall materials and wetting properties can be optimized based on this law.
4. Simulation studies on droplets with different physical properties have shown that the spreading trend of diesel droplets and water droplets under different wall contact angles is roughly the same. The smaller the wall contact angle, the larger the maximum spreading diameter of the droplets. Moreover, due to the influence of viscosity, the maximum spreading coefficient of diesel droplets under the same conditions is smaller than that of water droplets. From the perspective of evaporation rate, although the boiling point of diesel is generally around 210 ℃, much higher than the boiling point of water at around 100 ℃, the evaporation rate of water is lower than that of diesel under the same conditions due to the more hydrogen oxygen bonds in water.

REFERENCES

[1] *Shaopeng S,* Research on Spray Phase-Change Cooling Systems for High Heat Flux Electronic Components, ChongQing, School of Power Engineering, Chongqing University, 2010.
[2] *Meijuan L, Yuan L, Xishi W,* Experimental Study on the Impact of Single Droplet on Heated Birch Charcoal Surface, Journal of Chemical Engineering, Vol. 64, Iss. 08, pp. 2807-2812, 2019.

[3] *Lili W, Xiaoshu J,* Research Progress on Droplet Size in Wet Steam Two-Phase Flow in Turbines, Journal of Shanghai University of Science and Technology, Vol. 25, Iss. 4, pp. 30-312, 2004.
[4] *K. H. Seung, C. Jaewon, H. Nico, etal,* Metal nanoparticle direct inkjet printing for low-temperature 3D micro metal structure fabrication, Published by IOP Publishing, UK, Journal of Micromechanics and Microengineering, Vol. 20, Iss. 12, 125010, 2010.
[5] *S. Chandra, C. T. Avedisian,* On the collision of a droplet with a solid surface, Mathematical and Physical Sciences, Vol. 432, Iss. 1884, pp. 13-41, 1991.
[6] *L. G. Johann,* On the fixation of water in diverse fire, International Journal of Heat and Mass Transfer, Vol. 9, Iss. 11, 1153-1166, 1966.
[7] *K. Anders, N. Roth , A. Frohn,* The velocity change of ethanol droplets during collision with a wall analyse by image processing, Experiments influids, Vol. 15,Iss. 2, pp. 9l-96, 1993.
[8] *Wenbing Z, Longguang L, Tongxu Y,* Ring-Shaped Deposit Formation from the Evaporation of Solution Droplets, Acta Physica, Vol. 62, Iss. 19, 196102, 2019.
[9] *Bihao C,* translates to "The Effect of Substrate Thermal Properties on the Evaporation of Nanofluid Droplets, TianJin, translates to "School of Mechanical Engineering, Tianjin University of Commerce, 2014.
[10] *B. S. Gottfried, C. J. Lee, K. J. Bell,* The Leidenfrost phenomenon: film boiling of liquid droplets on a flat plate, International Journal of Heat and Mass Transfer, Vol. 9, Iss. 11, pp. 1167-1187, 1966.
[11] *L. H. J. Wachters,H. Bonne , H. J. van Nouhuis,* The heat transfer from a hot horizontal plate to sessile water drops in the sphprodial state, Chemical Engineering Science, Vol. 21, Iss. 10, pp. 923-936, 2021.
[12] *K, J, Baumeister, T. D. Hamill ,P. L. Schwartz, G. J. Schoessow,* Film boiling heat transfer to water drops on a flat plate, USA, Vol. 62, Iss. 64, pp. 52-61, 2021.
[13] *C. T. Avedisian, C. Ioffredo, M. J. O'Connor,* Film boiling of discrete droplets of mixtures of coal and water on a horizontal brass surface, Chemical Engineering Science, Vol. 39, Iss. 2, pp. 319-327, 1984.
[14] *M. Prat, P. Schmitz, D. Poulikakos,* On the effect of surface roughness on the vapor flow under Leidenfrost-levitated drop, Journal of fluids Engineering, Vol. 117, Iss. 3, pp. 519-525, 1995.
[15] A. *K. Sen, C. K. Law,* On a slowly evaporating droplet near a hot plate, International Journal of Heat and Mass Transfer, Vol. 27, Iss. 8, pp. 1418-1421, 1984.
[16] Gulyaev IP, Solonenko OP, Gulyaev PY, et al. Hydrodynamic features ofthe impact ofa hollow spherical drop on a flat surface. Technical Physics Letters, Vol.35,Iss. 10,pp.885-888,2009.
[4] *S. Sorohan, I. Manea, O. M. Constantinescu, N. Vasiliu*, FEM analysis of the composite materials used in civil buildings, U.P.B. Sci. Bull., Series D, Vol. **82**, Iss.4, 2020.
[5] *A.M. Schmitt, E. Miller, B. Engelmann, R. Batres, J. Schmitt,* G-code evaluation in CNC milling to predict energy consumption through Machine Learning, Advances in Industrial and Manufacturing Engineering, Vol. **8**, 2024, DOI: 10.1016/j.aime.2024.100140.
[6] *V. Gioncu, M. Ivan,* Teoria comportării critice şi postcritice a structurilor elastice (Theory of critical and post-critical behavior of elastic structures), Editura Academiei, Bucureşti, 1984.
[7] ***, ANSYS – Finite Element Analysis, Release 19.0 User Guide, 2018.